Desalination and Water Treatment
www.deswater.com
doi: 10.5004/dwt.2021.27194

225 (2021) 11–17
June

Preparation and application of flat-plate ceramic ultrafiltration membrane with high-performance by spray-dip coating method

Yahui Zhao, Yulong Yang, Qibing Chang*, Zhiwen Hu, Xiaozhen Zhang

School of Materials Science and Engineering, Jingdezhen Ceramic Institute, Jingdezhen 333403, China, Tel. +86-798-8499162; Fax: +86-798-8494973; email: changqb1258@hotmail.com (Q. Chang), Tel. +86-798-8499328; Fax: +86-798-8499328; email: Richard.zhao@foxmail.com (Y. Zhao), Tel. +86-798-8499162; Fax: +86-798-8494973; email: yyl0822@126.com (Y. Yang), Tel. +86-798-8499328; Fax: +86-798-8499328; email: 978236795@qq.com (Z. Hu), Tel. +86-798-8499328; Fax: +86-798-8499328; email: zhangxz05@126.com (X. Zhang)

Received 20 October 2020; Accepted 1 March 2021

ABSTRACT

A flat-plate ceramic ultrafiltration membrane with high permeability is prepared by a spray-dip coating method and one-step sintering. In the preparation process, the intermediate layer is prepared by spraying directly on the support even if the particle size of the powder is less than the pore size of the support. And then, the top separation layer is prepared by dipping the dried intermediate layer into the suspension and one-step co-sintering. The results show that the ceramic ultrafiltration membrane has an average pore size of 50 nm and a pure water flux of 725.74 L/(m^2 h bar). The rejection rate is 98.8% and the stable flux is 180 L/(m^2 h bar) in treating the stable 1,000 mg/L oil–water emulsion, which indicates the high permeability in treating oil-containing wastewater.

Keywords: Ceramic ultrafiltration membrane; Permeability; Rejection; Oil–water separation

1. Introduction

Ceramic membranes have the advantages of high porosity, high-temperature resistance, good corrosion resistance and high chemical stability [1,2]. Generally, the ceramic membrane possesses asymmetric structures: the support; intermediate layer and top separation layer [3,4] in which the pore size decrease following this order. To decrease the permeate resistance, the best choice is that the fine top separation is prepared directly on the coarse support, further reduce the thickness of the membrane. However, it is impossible because the fine particle of the coating slurry will fall into the pore in the support so that the top separation layer with defect-free is not formed.

Recently, a flat-plate ceramic membrane is given more attention due to its low permeate resistance originates from thin support. However, the thin support has a harmful effect on the flatness and the pore size distribution of the top separation membrane, especially the membrane is prepared by the dip-coating method [5] because the formation of the membrane layer depends on the capillary force of support and viscosity of the coating slurry [6–8]. The small thickness of the layer can only be formed due to the small suck time caused by the thin support. This small thickness results in the particles of slurry easily penetrate into the pores of the upper layer and require several layers to obtain the required pore size. This will inevitably lead to the increase of the permeate resistance.

Several methods [9,10] were adopted to solve the problem above mentioned. For example, thermal spraying was used to fabricate the Ti/TiO_2 separation layer with a small pore size straightly on the coarse support without an intermediate layer [11]. The sacrificial-interlayer or the network structure was adopted that derived

* Corresponding author.

from polyvinyl alcohol-boric acid complexion and cross-linking [12,13]. The above-mentioned methods contribute to decreasing the permeate resistance. However, the bonding strength between the top layer and the support is poor because the contact area is small caused by the lack of the intermediate layer.

In the present work, the thermal spray-dip coating method is adopted to prepare the ceramic ultrafiltration (UF) membranes with high-permeability straightly on the macroporous flat-plate support. The intermediate layer is prepared by spraying directly on the support in which the particle size of the powder is less than the pore size of the support. And then, the top separation layer is prepared by dipping the dried intermediate layer into the suspension and one-step co-sintering at 1,000°C for 2 h. The microstructure and the performance of the ceramic UF membranes were characterized.

2. Experimental

2.1. Materials

The Al_2O_3 flat-plate ceramic supports were fabricated by the extrusion method. The schematic of the flat-plate ceramic membrane is shown in Fig. 1. The average pore size of the support is 4 μm and the porosity is 40.37%.

Alumina (α-Al_2O_3) powders (d_{50} = 100 and 500 nm, purity ≥ 99%) were used to prepare the intermediate layer and top separation layer without further treatment.

2.2. Preparation of ultrafiltration membrane

The mass ratio of alumina powders: polyvinyl alcohol (PVA, 12 wt.%) solution: deionized water was 35:15:50. All of them were mixed by ball milling for 4 h. The stable 500 and 100 nm α-Al_2O_3 suspension was used for the spray-coating layer (intermediate layer) and dip-coating layer (separation layer), respectively.

The support was heated at a temperature of 60°C on the heating station, and then 500 nm alumina suspension was sprayed several times on the surface of the support. The water in the slurry was immediately evaporated by the heating station to form the spray-coating green layer. The spraying smoothness was controlled by the speed of the single-axis robotic, the spraying pressure and the spraying distance. During the special spray-coating process, the distance from the spray-coating device to the surface of support was 50 cm; the working gas pressure for spraying is 0.5 MPa; the slider of single-axis robotic was controlled by a computer at a speed of 0.12 m/s.

And then, the separation layer using 100 nm alumina suspension was fabricated straightly on the green spray-coating layer by the normal dip-coating method. The green UF membrane was dried in an oven at 80°C overnight. Finally, the UF flat-plate ceramic membrane was obtained after one-step co-sintering at 1,000°C for 2 h. The diagrammatic sketch of the preparation process is shown in Fig. 2.

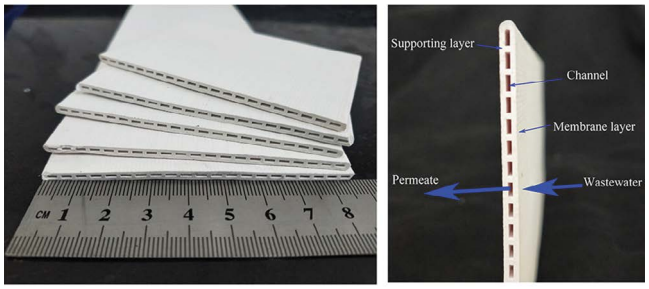

Fig. 1. Schematic of the Al_2O_3 ceramic flat-plate support.

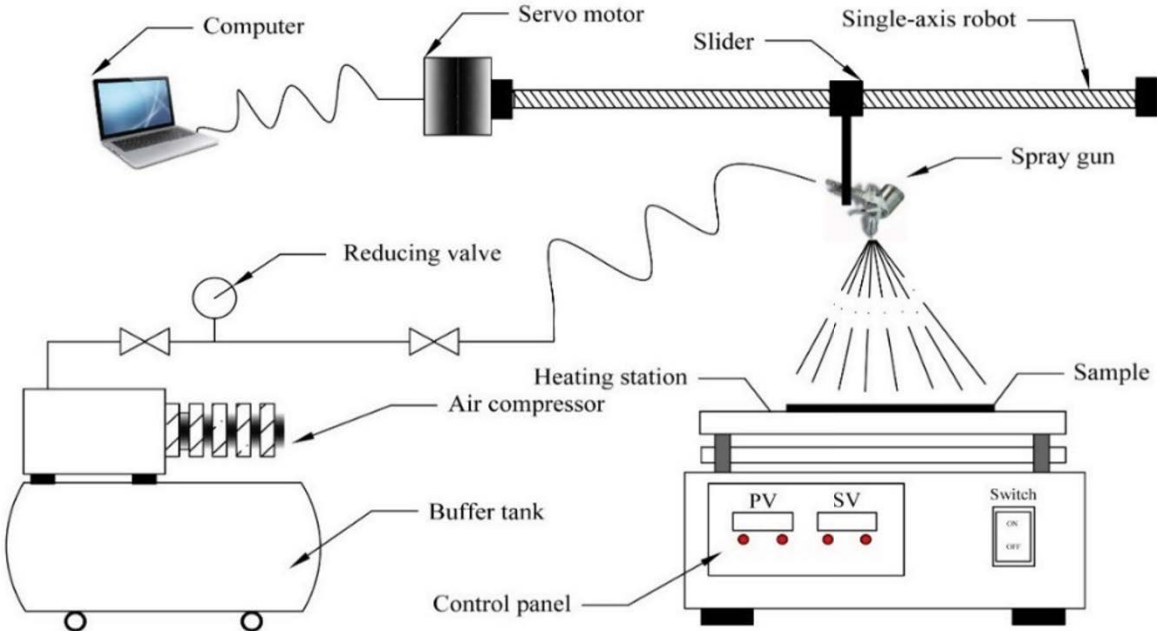

Fig. 2. Diagrammatic sketch of the thermal spray-coating process.

2.3. Characterization

The stable 1,000 mg/L oil–water emulsion was prepared as follows: petrol and Tween-80 (the weight petrol/Tween-80 ratio of 100:1) were mixed with deionized water at speed of 13,500 rpm for 5 min.

The surfaces and cross-sections of the UF samples were observed by field-emission scanning electron microscopy (FE-SEM; JSM-6700F, JEOL, Japan).

The pore size distribution of the UF samples was tested by a pore size distribution analyzer (PASA-20, China).

A home-made permeate device was used to test the water flux of the membrane.

The oil droplet size distribution of oil emulsion was measured by the laser diffraction particle size analyzer (Bettersize 2000, China).

The oil concentration of the permeate was determined by a UV spectrophotometer at a wavelength of 256 nm.

3. Results and discussion

3.1. Intermediate layer prepared by spraying method

Fig. 3 shows the FE-SEM images of the cross-section of the intermediate layer with different spraying mass. As can be seen, the thickness of the intermediate layer increases with the spraying mass. The thickness of the spray-coating layer increases from 13.5, 32.3, 64.7 to 146 μm corresponding to the spraying mass of 0.05, 0.10, 0.15 and 0.29 g.

As shown in Fig. 4, the thickness of the spray-coating layer increases along with the spraying mass and they are in a proportional relationship. This relationship can be formulated as: $y = 573.69x - 19.99$, in which y is the thickness (μm) and x is the spraying mass (g/cm^2). This equation is helpful to control the thickness of the ceramic membrane by spray mass. Specially, no particle seeps into the support even though the particle size of the particle in suspension (0.5 μm) is far lower than the pore size of the support (4 μm). It is benefited from the rapid solidification of the suspension when the suspension is sprayed on the hot support surface due to the evaporation of the solution in the suspension.

However, several holes distribute freely in the intermediate layer, which may be caused by the gas wrapped in the suspension during the spraying. If the hole has an open door in the intermediate layer surface, the defect is formed, as shown in Fig. 5.

Fig. 5 shows the FE-SEM images of the intermediate layer surface. The surface defects of the spray layer decrease with the increase of the spraying mass. When the spraying mass is 0.05 g/cm^2, there are many pin-holes on the surface

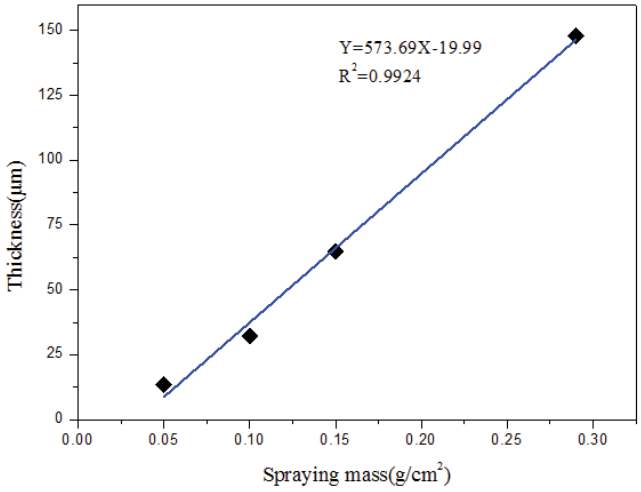

Fig. 4. Relationship of membrane thickness and spraying quality.

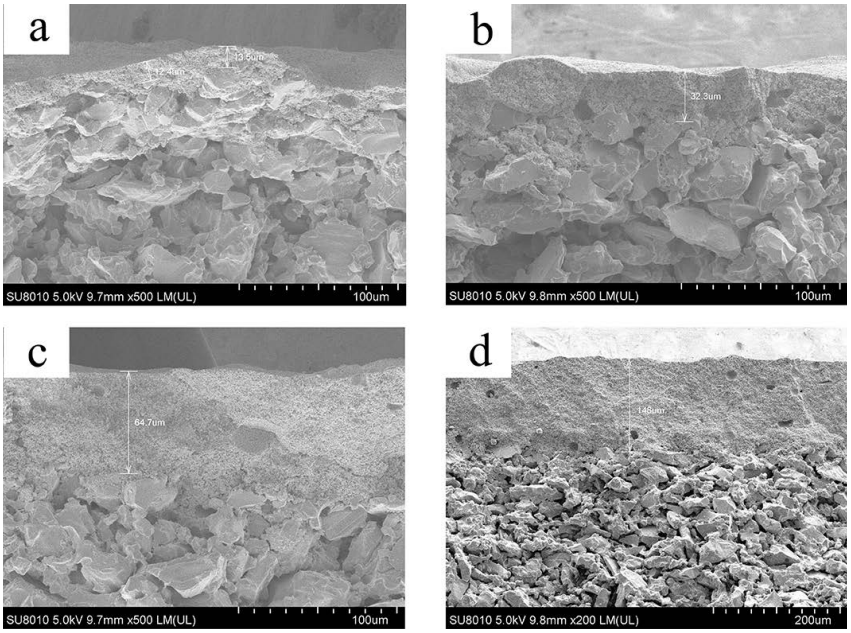

Fig. 3. FE-SEM images of the cross-section of the intermediate layer with different spraying mass: (a) 0.05 g/cm^2, (b) 0.10 g/cm^2, (c) 0.15 cm^2, and (d) 0.29 g cm^2.

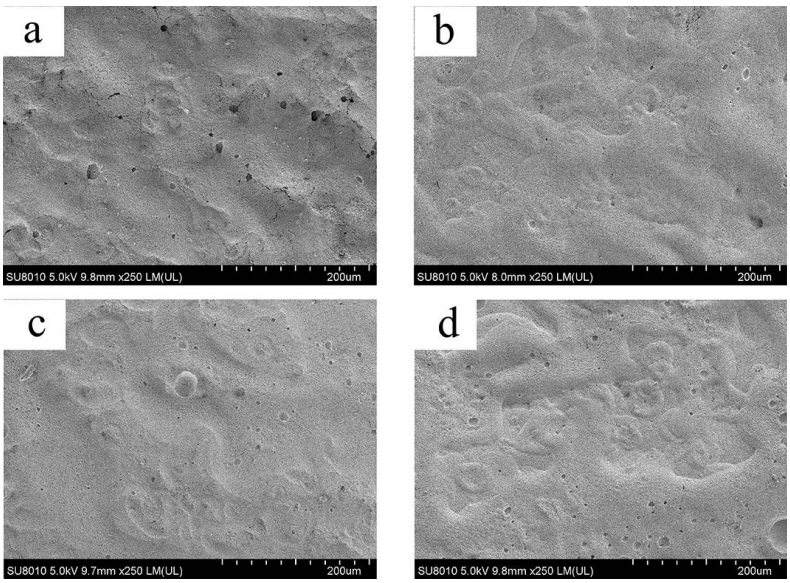

Fig. 5. FE-SEM images of the intermediate layer surface with different spraying mass: (a) 0.05 g/cm^2, (b) 0.10 g/cm^2, (c) 0.15 g/cm^2, and (d) 0.29 g/cm^2.

of the membrane (as shown in Fig. 5a). It may be explained that the escape velocity of the gas wrapped in the suspension is lower than the solidification of the suspension. The gas is wrapped in the layer. During the calcination process, the gas near the layer surface is broken and the pin-hole is formed. The evaporation of the solution decreases with the spraying mass due to the wet layer formed. The gas wrapped near the layer surface has enough time to escape. The opening hole will collapse and close. Only the crater-shaped bump is remained, as shown in Figs. 5b–d. It indicates that uneven layer surface can be obtained by a spraying method, which results easily in the membrane fouling.

Wide pore size distribution reflects the bad accumulation of the particle and the serious membrane defect. The pore size distribution of intermediate layer surface with different spraying mass is shown in Fig. 6. The mean pore size of the intermediate layer decreases gradually with the increase of the spraying mass from 0.05 to 0.2 g. Meanwhile, the pore-size distribution changes narrow and the largest pore-size decreases. For ceramic membrane, the membrane pore is formed by the accumulation of particles. According to the measuring principle of membrane pore, the tortuous membrane pores are regards as a bound of capillaries. The pore tortuosity increases with the increase of the membrane layer thickness [6]. Therefore, the mean pore-size of the intermediate layer decreases with the layer thickness. For the spraying mass is 0.05 g/cm^2, the thickness is so thin that the spraying layer cannot cover completely the support surface. The relatively large maximum membrane pore indicates the existence of the membrane defect.

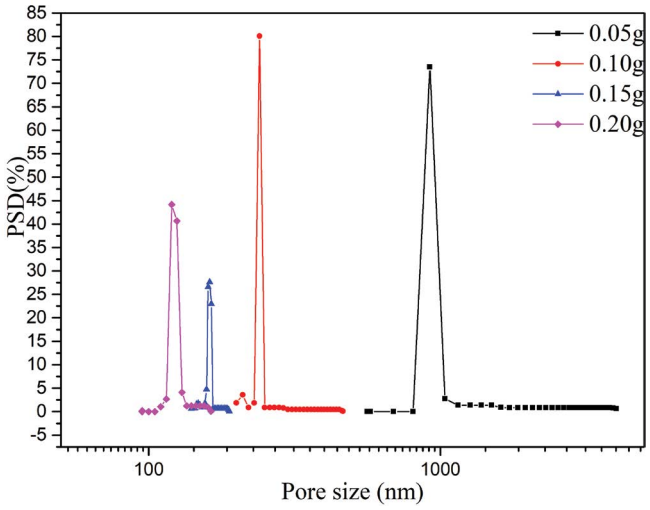

Fig. 6. Pore size distribution of the intermediate layer with different spraying mass.

3.2. Top separation layer prepared by dip-coating method

Due to the lack of the spreading of the suspension on the layer surface, it is impossible to obtain the smooth layer surface by a spraying method, but dip-coating can do it. Fig. 7 shows the FE-SEM images of the cross-section of the UF membrane with different dip-coating times. When the dip-coating time increases from 5 to 20 s, the thickness of the separation layer increases from 7.7 to 22.4 μm, but then down to 20.2 μm. Because the dip-coating method is based on the capillary force of the support and the concentration of coating slurry. The capillary force disappears with the dip-coating time increased and the membrane thickness decreased due to the difference in concentration of slurry. In fact, the thickness of the wet membrane can be controlled by the dipping time and the viscosity of the suspension [4].

What needs to be said is that the thickness of the top layer is uniform despite that the top layer is winding caused by the uneven intermediate layer surface. Fig. 7a shows the UF membrane surface is smooth compared with the spray layer. The smooth membrane surface can effectively

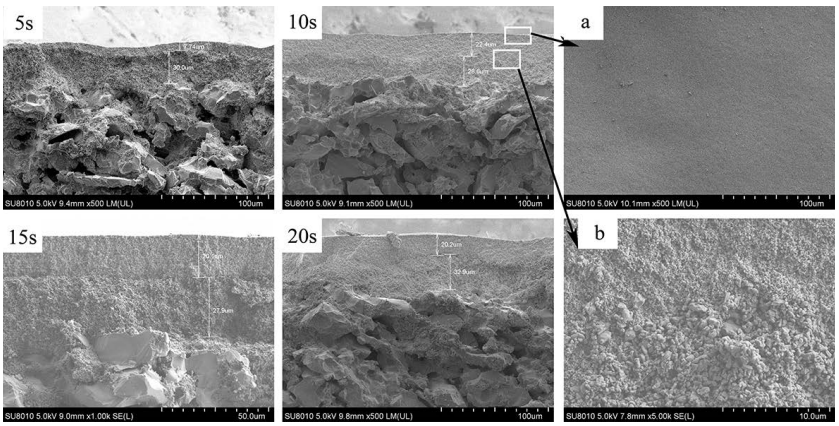

Fig. 7. FE-SEM images of the cross-section of UF membrane with different dipping times.

reduce membrane fouling during cross-flow filtration and backwashing, which improves the separation performance [8]. Meanwhile, good combination exists between the spray layer and the dip-coating layer, as shown in Fig. 7b. The clear boundary indicates that 100 nm Al_2O_3 particles do not penetrate into the spray green layer. It means that the spray layer and the dip-coating layer can be prepared together, and then co-sintered only once, which contributes to decrease the ceramic membrane cost.

Fig. 8 shows the pore size distributions of the ceramic UF membrane with different dipping times. As can be seen, the top layers prepared by different dipping times have similar mean pore sizes. However, the biggest pore size of the ceramic membrane decreased with the dipping time increased. Especially, the dip-coating time is 5 s, the pore-size distribution is wide and the biggest pore reaches 150 nm, indicating that more membrane defects exist. If the dipping time is over 10 s, the thickness of the membrane layer increases compared to the dipping time of 5 s. The pore size distribution changes narrow and the biggest pore-size is reduced.

3.3. Permeability of UF membrane

3.3.1. Pure water

As above discussed, the optimized preparation condition is that the spraying mass is 0.10 g/cm^2, the dipping time is 10 s. The scanning electron microscopy images of the cross-section and the surface of the UF membrane are shown in Fig. 7 marked as 10 s. The permeability of ceramic UF membrane is tested by a home-made permeate device and the pure water flux is 725.74 L/(m^2 h bar).

Table 1 lists the water flux of the membranes in this work and in literature. The ceramic UF membranes prepared by the spray-dipping method have a higher pure water flux than the other reported in literature [8,9,14–19], which is mainly due to the support have a pore size of 4 μm and the total thickness of both layers is about 50 μm.

3.3.2. Oil–water emulsion

The permeate flux and the oil rejection of the UF membrane are shown in Fig. 9. At the beginning of filtration, the flux of the membrane drops sharply, and then the curve tends to stable. The decrease of the filtration flux is due to the concentration polarization [20–22] and membrane fouling [23,24]. Concentration polarization is attributed to the rapid increase of the oil droplets concentration near the membrane surface. Membrane fouling is due to the deposition and adsorption of oil droplets on the surface or in the pores of the membrane [25,26]. The process of the concentration polarization and membrane fouling tends to the equilibrium after 60 min, which is reflected by the stable permeate flux. Under the stable operation conditions, the

Table 1
Water permeability of the membranes and in literatures

Materials	Average pore size (nm)	Water permeability (L/(m^2 h bar))	References
TiO_2	100–120	740	Wang et al. [8]
Al_2O_3	130	550	Song et al. [14]
Polysulfone-g-Polyethylene glycol (PSF-g-PEG)	51	139	Yuan et al. [15]
Fly ash/Al_2O_3	100	445	Zou et al. [9]
TiO_2	50	117	Oun et al. [16]
TiO_2	72	33 ± 2	Bouazizi et al. [17]
TiO_2	108	700	Ke et al. [18]
Al_2O_3	300	500	Wang et al. [19]
Al_2O_3	50 ± 5	725.74	This work

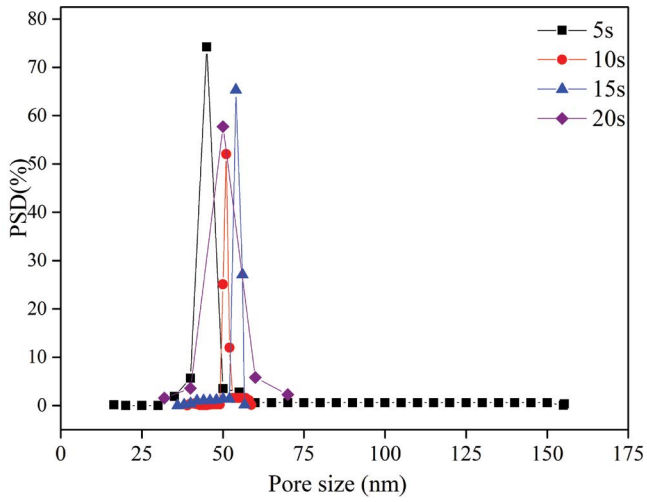

Fig. 8. Pore-size distribution of the top separation layers with different dipping times.

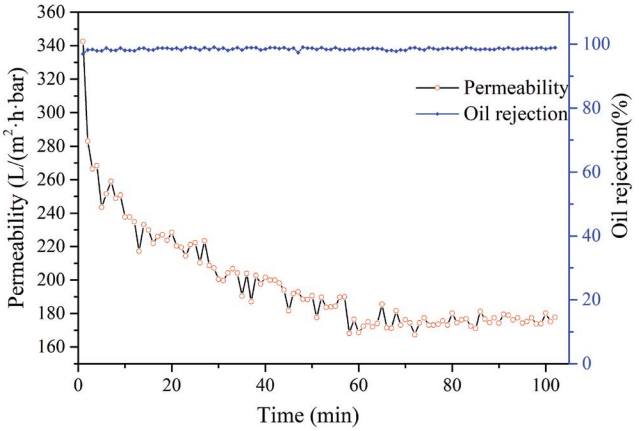

Fig. 9. Permeate flux and rejection rate of the UF membrane treating stable 1 g/L emulsion.

oil rejection rate is about 98.5% and the stable flux is 180 L/(m² h bar) under the trans-membrane pressure of 0.5 bar.

As shown in Fig. 10, the feed (stable oil–water emulsion) is a white liquid, however, the permeate is clear and transparent. It indicates that the ceramic UF membrane can separate effectively the high oil concentration emulsion.

Fig. 10. Photograph of the feed and the permeate.

Table 2 lists the separation performance of oil–water emulsion compared with the results reported in the literatures [27–30]. The ceramic UF membrane in this work has good parameters in oil rejection rate and permeability, which exhibits a great potential application in wastewater treatment.

4. Conclusions

A novel spray-dip coating method is adopted to prepare a flat-plate ceramic ultrafiltration membrane with high permeability. In the preparation process, the intermediate layer is prepared by spraying directly on the support using fine powder. And then, the top separation layer is prepared by dipping the dried intermediate layer into the suspension and one-step co-sintering.

The dip-coating layer with a relatively smooth surface can be prepared straightly on the uneven green spray-coating layer. After co-sintering at 1,000°C for 2 h, the obtained ceramic membrane has the membrane thickness of 50 μm, the average pore size of 50 nm and the pure water flux of 725.74 L/(m² h bar).

The ceramic UF membrane has high separation properties with an oil rejection rate of 98.8% and a stable permeate flux of 180 L/(m² h bar) during the oil concentration of 1,000 mg/L and the working pressure of 0.5 bar.

Acknowledgments

The authors gratefully acknowledge the financial support from the National Natural Science Foundation of China

Table 2
Separation performance of oil–water emulsion in this work and in literature

Material	Pore size (μm)	Oil concentration (mg/L)	Stable permeability (L/(m² h bar))	Oil rejection (%)	References
TiO_2-Mullite	0.11	200	150	97_{TOC}	[27]
Al_2O_3	0.05	500	63.9	98.1	[28]
Yttria-stabilized Zirconia – Carbon nanotubes (YSZ-CNT)	0.7	210	36	100	[29]
Polysulfone	0.1	78	76	95	[30]
Al_2O_3	0.05	1,000	180	98.8	This work

(No.21761015, 51662020 and 51772136), Jiangxi Province Department of Science and Technology (No. 20165BCB19014), Jiangxi Province education Department (No. GJJ190737).

References

[1] Q. Chang, Y. Yang, X. Zhang, Y. Wang, J.-e. Zhou, X. Wang, S. Cerneaux, L. Zhu, Y. Dong, Effect of particle size distribution of raw powders on pore size distribution and bending strength of Al_2O_3 microfiltration membrane supports, J. Eur. Ceram. Soc., 34 (2014) 3819–3825.
[2] L. Zhu, X. Dong, M. Xu, F. Yang, M.D. Guiver, Y. Dong, Fabrication of mullite ceramic-supported carbon nanotube composite membranes with enhanced performance in direct separation of high-temperature emulsified oil droplets, J. Membr. Sci., 582 (2019) 140–150.
[3] X. Yin, K. Guan, P. Gao, C. Peng, J. Wu, A preparation method for the highly permeable ceramic microfiltration membrane – precursor film firing method, RSC Adv., 8 (2018) 2906–2914.
[4] Q. Chang, R. Peng, X. Liu, D. Peng, G. Meng, A modified rate expression of wet membrane formation from ceramic particles suspension on porous substrate, J. Membr. Sci., 233 (2004) 51–58.
[5] W. Zhu, Y. Liu, K. Guan, C. Peng, W. Qiu, J. Wu, Integrated preparation of alumina microfiltration membrane with super permeability and high selectivity, J. Eur. Ceram. Soc., 39 (2019) 1316–1323.
[6] M. Qiu, S. Fan, Y. Cai, Y. Fan, N. Xu, Co-sintering synthesis of bi-layer titania ultrafiltration membranes with intermediate layer of sol-coated nanofibers, J. Membr. Sci., 365 (2010) 225–231.
[7] A.Y. Kirschner, Y.-H. Cheng, D.R. Paul, R.W. Field, B.D. Freeman, Fouling mechanisms in constant flux crossflow ultrafiltration, J. Membr. Sci., 574 (2019) 65–75.
[8] Y.H. Wang, X.Q. Liu, G.Y. Meng, Preparation and properties of supported 100% titania ceramic membranes, Mater. Res. Bull., 43 (2008) 1480–1491.
[9] D. Zou, M. Qiu, X. Chen, E. Drioli, Y. Fan, One step co-sintering process for low-cost fly ash based ceramic microfiltration membrane in oil-in-water emulsion treatment, Sep. Purif. Technol., 210 (2019) 511–520.
[10] D. Zou, M. Qiu, X. Chen, Y. Fan, One-step preparation of high-performance bilayer α-alumina ultrafiltration membranes via co-sintering process, J. Membr. Sci., 524 (2017) 141–150.
[11] Y. Lin, D. Zou, X. Chen, M. Qiu, H. Kameyama, Y. Fan, Low temperature sintering preparation of high-permeability TiO_2/Ti composite membrane via facile coating method, Appl. Surf. Sci., 349 (2015) 8–16.
[12] W. Qin, K. Guan, B. Lei, Y. Liu, C. Peng, J. Wu, One-step coating and characterization of α-Al_2O_3 microfiltration membrane, J. Membr. Sci., 490 (2015) 160–168.
[13] W. Qin, C. Peng, J. Wu, A sacrificial-interlayer technique for single-step coating preparation of highly permeable alumina membrane, Ceram. Int., 43 (2017) 901–904.
[14] I.-H. Song, B.-S. Bae, J.-H. Ha, J. Lee, Effect of hydraulic pressure on alumina coating on pore characteristics of flat-sheet ceramic membrane, Ceram. Int., 43 (2017) 10502–10507.
[15] T. Yuan, J. Meng, T. Hao, Y. Zhang, M. Xu, Polysulfone membranes clicked with poly (ethylene glycol) of high density and uniformity for oil/water emulsion purification: effects of tethered hydrogel microstructure, J. Membr. Sci., 470 (2014) 112–124.
[16] A. Oun, N. Tahri, S. Mahouche-Chergui, B. Carbonnier, S. Majumdar, S. Sarkar, G.C. Sahoo, R. Ben Amar, Tubular ultrafiltration ceramic membrane based on titania nanoparticles immobilized on macroporous clay-alumina support: elaboration, characterization and application to dye removal, Sep. Purif. Technol., 188 (2017) 126–133.
[17] A. Bouazizi, M. Breida, A. Karim, B. Achiou, M. Ouammou, J.I. Calvo, A. Aaddane, K. Khiat, S.A. Younssi, Development of a new TiO_2 ultrafiltration membrane on flat ceramic support made from natural bentonite and micronized phosphate and applied for dye removal, Ceram. Int., 43 (2017) 1479–1487.
[18] X.B. Ke, H.Y. Zhu, X.P. Gao, J.W. Liu, Z.F. Zheng, High-performance ceramic membranes with a separation layer of metal oxide nanofibers, Adv. Mater., 19 (2007) 785–790.
[19] P. Wang, P. Huang, N. Xu, J. Shi, Y. Lin, Effects of sintering on properties of alumina microfiltration membranes, J. Membr. Sci., 155 (1999) 309–314.
[20] J. Lin, C.Y. Tang, W. Ye, S.-P. Sun, S.H. Hamdan, A. Volodin, C.V. Haesendonck, A. Sotto, P. Luis, B. Van der Bruggen, Unraveling flux behavior of superhydrophilic loose nano-filtration membranes during textile wastewater treatment, J. Membr. Sci., 493 (2015) 690–702.
[21] H. Rezaei, F.Z. Ashtiani, A. Fouladitajar, Effects of operating parameters on fouling mechanism and membrane flux in cross-flow microfiltration of whey, Desalination, 274 (2011) 262–271.
[22] Y. Zhu, D. Chen, Novel clay-based nanofibrous membranes for effective oil/water emulsion separation, Ceram. Int., 43 (2017) 9465–9471.
[23] J. Lin, W. Ye, H. Zeng, H. Yang, J. Shen, S. Darvishmanesh, P. Luis, A. Sotto, B. Van der Bruggen, Fractionation of direct dyes and salts in aqueous solution using loose nanofiltration membranes, J. Membr. Sci., 477 (2015) 183–193.
[24] J. Lin, W. Ye, M.-C. Baltaru, Y.P. Tang, N.J. Bernstein, P. Gao, S. Balta, M. Vlad, A. Volodin, A. Sotto, P. Luis, A.L. Zydney, B. Van der Bruggen, Tight ultrafiltration membranes for enhanced separation of dyes and Na_2SO_4 during textile wastewater treatment, J. Membr. Sci., 514 (2016) 217–228.
[25] Q. Chang, J.-e. Zhou, Y. Wang, J. Liang, X. Zhang, S. Cerneaux, X. Wang, Z. Zhu, Y. Dong, Application of ceramic microfiltration membrane modified by nano-TiO_2 coating in separation of a stable oil-in-water emulsion, J. Membr. Sci., 456 (2014) 128–133.
[26] Y. Zhu, W. Xie, F. Zhang, T. Xing, J. Jin, Interfaces, Superhydrophilic in-situ-cross-linked zwitterionic poly-electrolyte/PVDF-blend membrane for highly efficient oil/water emulsion separation, ACS Appl. Mater. Interfaces, 9 (2017) 9603–9613.
[27] F.L. Hua, Y.F. Tsang, Y.J. Wang, S.Y. Chan, H. Chua, S.N. Sin, Performance study of ceramic microfiltration membrane for oily wastewater treatment, Chem. Eng. J., 128 (2007) 169–175.
[28] X. Chen, L. Hong, Y. Xu, Z.W. Ong, Ceramic pore channels with inducted carbon nanotubes for removing oil from water, ACS Appl. Mater. Interfaces, 4 (2012) 1909–1918.
[29] A. Salahi, A. Gheshlaghi, T. Mohammadi, S.S. Madaeni, Experimental performance evaluation of polymeric membranes for treatment of an industrial oily wastewater, Desalination, 262 (2010) 235–242.
[30] L. Zhu, M. Chen, Y. Dong, C.Y. Tang, A. Huang, L. Li, A low-cost mullite-titania composite ceramic hollow fiber microfiltration membrane for highly efficient separation of oil-in-water emulsion, Water Res., 90 (2016) 277–285.